Super-Effective-Field Theory of Chiral Orders in the Two-Dimensional Heisenberg Model(MASTER THESIS)

AUTHOR(S):

KAWARABAYASHI, TOHRU

CITATION:

KAWARABAYASHI, TOHRU. Super-Effective-Field Theory of Chiral Orders in the Two-Dimensional Heisenberg Model(MASTER THESIS). 物性研究 1990, 55(2): 226-258

ISSUE DATE:

1990-11-20

URL:

http://hdl.handle.net/2433/94364

物性研究55－2(1990－11)

修士論文　(1989年度)

超有効場理論による二次元ハイゼンベルグ模型における カイラルオーダーの解析

東京大学　理学部　　河原林　透

要旨

この論文では、二次元反強磁性ハイゼンベルグ模型において二つのカイラルオーダー、スカラー型カイラルオーダーとベクトル型カイラルオーダー、についてその相転移の可能性を調べた。第一章では、鈴木によって考案された超有効場理論を用いてスカラー型カイラルオーダーについて議論した。超有効場理論は平均場理論の一般化であり、強相関の系やエキゾチックな相転移を扱うのに有効であると考えられ、既にスピングラスやベクトル型カイラルオーダーに応用されている。また、第二章ではベクトル型カイラルオーダーについて解析的手法により厳密な結果を得た。いずれの場合も超有効場という考えが重要な役割を果たしている。

第一章

この章では、スカラー型カイラルオーダーについて調べた。スカラー型カイラルオーダーとは（$\boldsymbol{S}_i \cdot (\boldsymbol{S}_j \times \boldsymbol{S}_k)$）で定義され、最近 Wen, Wilczek, Zee らによってその相転移の可能性が提案された。ここでは次近接相互作用をもつ二次元正方格子上のスピン１／２反強磁性ハイゼンベルグ模型を考え、この系においてスカラー型カイラルオーダーの相転移が起こるかどうかを超有効場理論を用いて調べた。また、次近接相互作用によって導入されたフラストレーションの効果についても調べた。その結果、この系ではカイラルオーダーの相関が弱く、これまでの計算結果からは相転移の兆候は見られなかった。また、次近接相互作用を大きくするとカイラルオーダーの相関が抑えられる傾向が見られた。

第二章

この章では、ベクトル型カイラルオーダーについて調べた。ベクトル型カイラルオーダーは$(\boldsymbol{S}_i \times \boldsymbol{S}_j + \boldsymbol{S}_j \times \boldsymbol{S}_k + \boldsymbol{S}_k \times \boldsymbol{S}_i)$で定義される。この場合には、ボゴリューボフ（Bogoliubov）不等式を用いることによって、短距離相互作用をもつ二次元ハイゼンベルグ模型においては、有限温度でベクトル型カイラルオーダーが存在しないことが厳密に示された。正方格子と三角格子の場合についての具体的な証明が示してある。

MASTER THESIS

Super-Effective-Field Theory of Chiral Orders in the Two-Dimensional Heisenberg Model

TOHRU KAWARABAYASHI

Department of Physics, Faculty of Science, University of Tokyo

January 1990

Contents

I Scalar Chiral Order 230
1 Introduction 230
2 Scalar Chiral Order 230
2.1 Review 230
2.2 Properties of the scalar chiral order 231
3 Super-Effective-Field Theory (SEFT) of the Scalar Chiral Order . . . 233
3.1 General Formalism 233
3.2 Bethe-like approximation 236
4 Numerical Calculations 238
4.1 4-Spin Cluster Approximation 238
4.2 6-Spin Cluster Approximation 241
4.3 12-Spin Cluster Approximation 243
5 Discussion 245

II Vector Chiral Order 247
1 Introduction 247
2 Absence of the Vector Chiral Order in the Two-Dimensional Heisenberg Model 248

A Fermionic Representation of the Scalar Chiral Order 250

B Properties of the Scalar Chiral Order X_{ijk} 254

C Analytic Results in a System of Four Spins 255

References 257

Acknowledgements

I would like to express my gratitude to Professor Masuo Suzuki for stimulating discussions and encouragement.

I would like to thank Mr. Naoki Kawashima, Mr. Nobuo Furukawa and Dr. Kenji Yonemitsu for stimulating discussions and a great deal of valuable advice. I would thank Dr. Mokoto Katori, Dr. Akira Terai, Mr. Nobuyasu Ito, Yoshihiko Nonomura and all other members of Suzuki research group and Wada research group for helpful suggestions.

This study is partially financed by the Research Fund of the Ministry of Education, Science and Culture. The numerical calculations were done on the HITAC M 680H/M 682H and HITAC S-820/80 of the Computer Center, University of Tokyo.

Chapter I

Scalar Chiral Order

1 Introduction

It is a very interesting problem to study chiral orders in the two-dimensional frustrated quantum spin systems, especially for the understanding of high-T_c superconductors[1]. Recently a new chiral order, namely scalar chiral order, was proposed by Wen, Wilckzek and Zee.[2,3]. The scalar chiral order which is defined by $\boldsymbol{S}_i \cdot (\boldsymbol{S}_j \times \boldsymbol{S}_k)$ breaks the parity (P) and the time reversal (T) symmetry.

We have studied the scalar chiral order in the two-dimensional spin 1/2 Heisenberg model by using the super-effective-field theory, which was proposed by Suzuki[4]. The super-effective-field theory, being a generalization of the mean field approximation, is very useful to study exotic phase transitions in strongly correlated systems. It has been already applied to vector chiral orders[4,5] and spin glasses[4,6]. Together with the coherent-anomaly method (CAM)[7,8], it reveals the non-classical critical behavior of such exotic phase transitions. In the present paper, we apply SEFT to scalar chiral orders in the quantum Heisenberg model to investigate the possibility of chiral phase transitions.

2 Scalar Chiral Order

2.1 Review

Recently Wen, Wilckzek and Zee(W. W. Z.)[2] pointed out the possibility of a new kind of symmetry breakdown in the two-dimensional antiferromagnetic Heisenberg model. It is the emergence of the non-zero expectation value of the scalar chiral order $X_{i,j,k} = \boldsymbol{S}_i \cdot (\boldsymbol{S}_j \times \boldsymbol{S}_k)$, which implies the parity(P) and the time reversal(T) symmetry breaking. W. W. Z. considered the antiferromagnetic Heisenberg model on the two-dimensional square lattice with next nearest neighbor interactions, and they suggested, by using the fermionic mean field theory, that "the chiral spin liquid state" characterized by $\langle X_{i,j,k} \rangle \neq 0$ is a possible ground state .

Baskaran[9] studied the scalar chiral order for the triangular lattice case. He introduces the pseudo scalar variables m_{ijk} by using the functional integral method, and expands the free energy in powers of m. Based on the symmetry of the free energy as a function of m, Baskaran suggests that the symmetry breakdown does

not occur if the next nearest neighbor interactions are absent, but that if the next nearest neighbor interactions are present there may be an Ising like phase transition.

There are also numerical calculations in small lattices about the scalar chiral order. Imada[10] calculated the expectation value of the square of the scalar chiral order at the ground state of the Heisenberg model, and suggested that the correlation is too small for the existence of the chiral order. Dagotto and Moreo[11] calculated the expectation values of several order parameters, including the scalar chiral order, at the ground state of the two-dimensional Heisenberg model with next nearest neighbor interactions. They measure also the square of the scalar chiral order, but there is no indication of its existence.

2.2 Properties of the scalar chiral order

Let us consider the expectation value of the scalar chiral order defined by

$$E_{ijk} \equiv \langle \sigma_i \cdot (\sigma_j \times \sigma_k) \rangle = 8 \cdot \langle X_{ijk} \rangle \tag{2.1}$$

where ${}^t\sigma = (\sigma^x, \sigma^y, \sigma^z)$ denote the Pauli matrices[2]. We rewrite E_{ijk} in the fermionic representation. We then have the following relations(Appendix A)

$$Pl_{123} - Pl_{132} = \frac{i}{2} E_{123} \tag{2.2}$$

$$Pl_{1234} - Pl_{1432} = \frac{i}{4}(E_{123} + E_{134} + E_{124} - E_{234}) \tag{2.3}$$

where

$$Pl_{ijk} \equiv \langle \chi_{ij}\chi_{jk}\chi_{ki} \rangle \tag{2.4}$$

$$Pl_{ijkl} \equiv \langle \chi_{ij}\chi_{jk}\chi_{kl}\chi_{li} \rangle \tag{2.5}$$

$$\text{and} \quad \chi_{ij} \equiv \sum_\sigma c^\dagger_{i\sigma} c_{j\sigma} \tag{2.6}$$

Here $c^\dagger_{i\sigma}(c_{i\sigma})$ is a creation(annihilation) operator of an electron with spin σ on site i, and the brackets denote the thermal average. In deriving eq.(2.2) and eq.(2.3), we have used the following relations:

$$\begin{cases} S^+_i = \frac{1}{2}\sigma^+_i = c^\dagger_{i\uparrow} c_{i\downarrow} \\ S^-_i = \frac{1}{2}\sigma^-_i = c^\dagger_{i\downarrow} c_{i\uparrow} \\ S^z_i = \frac{1}{2}\sigma^z_i = \frac{1}{2}(c^\dagger_{i\uparrow} c_{i\uparrow} - c^\dagger_{i\downarrow} c_{i\downarrow}). \end{cases} \tag{2.7}$$

It is to be noted that eq.(2.2) is satisfied as an operator identity, but eq.(2.3) is satisfied under the constraint $\sum_\sigma n_{i\sigma} = 1$ i. e. , the half-filled condition.

The quantity χ_{ij} is an operator which transports an electron on site j to site i. Thus Pl_{123} is the expectation value for the electron hopping around the loop(123) in

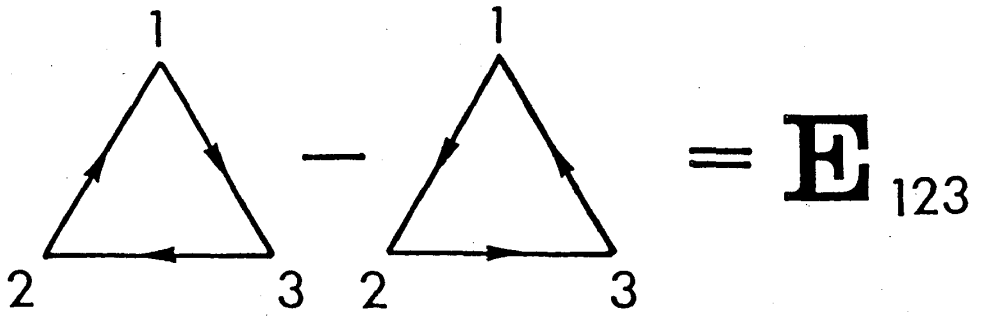

Fig. 1.1: Closed loop(123).

the direction $1 \to 3 \to 2 \to 1$. Therefore eq.(2.2) means that the expectation value of the scalar chiral order (E_{123}) is the difference between the expectation values for the hopping around the closed loop(123) in opposite directions(Fig.1.1).

The existence of the expectation value of the scalar chiral order (E_{123}) can be regarded as the fact that there is a flux through the loop(123). The relation between E_{ijk} and the Berry phase is also discussed by W. W. Z. [2].

The following remarkable properties of the scalar chiral order X_{123} was pointed out[2](Appendix B):

$$X_{123}^2 = -\frac{1}{16}(\boldsymbol{S}_1 + \boldsymbol{S}_2 + \boldsymbol{S}_3)^2 + \frac{15}{64} \quad , \quad \text{and} \tag{2.8}$$

$$[X_{123}, \boldsymbol{S}] = 0 \quad , \text{where} \quad \boldsymbol{S} = \boldsymbol{S}_1 + \boldsymbol{S}_2 + \boldsymbol{S}_3. \tag{2.9}$$

Because of eq.(2.9), both the chiral order X_{123} and the total spin $\boldsymbol{S}$ can be diagonalized simultaneously. It is easily seen from eq.(2.8) that the total spin $S = 3/2$ states are the eigenstates of X_{123} with eigenvalue 0. Let us consider the total spin $S = 1/2$ states. There are two different spin 1/2 states denoted by $|S = 1/2, S_z\rangle^+$ and $|S = 1/2, S_z\rangle^-$[2]. The + states $|S = 1/2, S_z = \pm 1/2\rangle^+$ are explicitly given as follows,

$$|S = 1/2, S_z = 1/2\rangle^+ = \frac{1}{\sqrt{3}}(|\uparrow\uparrow\downarrow\rangle + \omega|\uparrow\downarrow\uparrow\rangle + \omega^2|\downarrow\uparrow\uparrow\rangle) \tag{2.10}$$

$$|S = 1/2, S_z = -1/2\rangle^+ = -\frac{1}{\sqrt{3}}(|\downarrow\downarrow\uparrow\rangle + \omega|\downarrow\uparrow\downarrow\rangle + \omega^2|\uparrow\downarrow\downarrow\rangle) \tag{2.11}$$

where ω denotes the cube root of unity so that $1 + \omega + \omega^2 = 0$. The $-$ states $|S = 1/2, S_z = \pm 1/2\rangle^-$ are obtained from (2.10) and (2.11) by replacing ω by ω^2. We see that $|S = 1/2, S_z\rangle^+$ is an eigenstate of X_{123} with the eigenvalue $-\sqrt{3}/4$, and $|S = 1/2, S_z\rangle^-$ is an eigenstate with the eigenvalue $\sqrt{3}/4$.

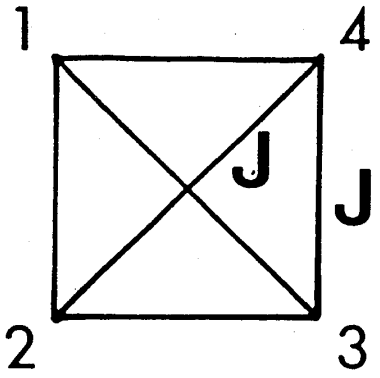

Fig. 1.2: The plaquette we consider.

We can construct two spin singlet states corresponding to the above two spin 1/2 states by adding the forth spin. It is easily shown that the total spin singlet states are given by

$$|S=0\rangle^{\alpha} = |S=1/2, S_z=1/2\rangle^{\alpha} \otimes |\downarrow\rangle - |S=1/2, S_z=-1/2\rangle^{\alpha} \otimes |\uparrow\rangle \qquad (2.12)$$

for $\alpha = \pm 1$. Thus $|S=0\rangle^{\alpha}$ is an eigenstate of X_{123} with a non-zero eigenvalue,

$$X_{123}|S=0\rangle^{\alpha} = -\frac{\sqrt{3}}{4}\alpha|S=0\rangle^{\alpha}. \qquad (2.13)$$

If we consider the following Hamiltonian:

$$H \equiv J(\boldsymbol{S}_1+\boldsymbol{S}_2+\boldsymbol{S}_3+\boldsymbol{S}_4)^2, \qquad (2.14)$$

for $J>0$, the ground state is a spin singlet state $|S=0\rangle^{\alpha}$ for $\alpha=\pm 1$. Therefore, in this 4-spin system, the ground states have the Ising-like $\pm$ degeneracy with respect to the eigenvalues of X_{123}. It should be noted that the Hamiltonian (2.14) is equivalent to the Heisenberg Hamiltonian with the next nearest neighbor interaction ; the strength of which is equal to that of the nearest neighbor ones(Fig.1.2). In section 3, we will see that this degeneracy of ground states in a four-spin system occurs only in the case where the strength of n.n.n. and n.n. interactions are equal. In other cases the ground state is unique and symmetric even if the n.n.n. interactions are present.

3 Super-Effective-Field Theory (SEFT) of the Scalar Chiral Order

3.1 General Formalism

The Hamiltonian we consider here is the antiferromagnetic Heisenberg Hamiltonian with next nearest neighbor interactions:

$$\mathcal{H} = \sum_{n.n.} J\boldsymbol{S}_i \cdot \boldsymbol{S}_j + \sum_{n.n.n.} J'\boldsymbol{S}_i \cdot \boldsymbol{S}_j \qquad (3.1)$$

where $J(>0)$ and $J'(>0)$ are the nearest neighbor and next nearest neighbor couplings, respectively. The next nearest neighbor coupling ($J'>0$) introduces frustrations in this system.

In order to construct the mean-field-type approximation, we consider the cluster (Ω) shown in Fig.1.3. The elementary domain D_j is a triangular or square plaquette in which the scalar chiral order parameter Q_j is defined. The domain D_0 is the one which lies in the center of the cluster Ω and the other domains $D_1, D_2, \ldots, D_z \in \partial\Omega$ are the boundaries of the cluster.

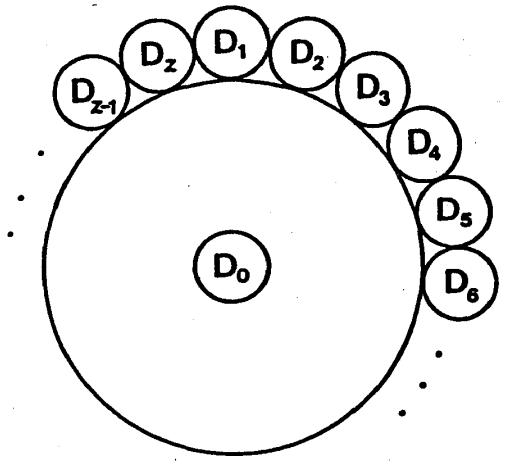

Fig. 1.3: The cluster Ω.

Then following Suzuki[4] we consider the following effective Hamiltonian:

$$\mathcal{H}_{eff} = \mathcal{H}_\Omega - \sum_{k\in\partial\Omega} \Lambda_k Q_k \quad , \tag{3.2}$$

where $\mathcal{H}_\Omega$ is the Heisenberg Hamiltonian (3.1) in the cluster Ω, Λ_k is a super-effective-field conjugate to the chiral order parameter Q_k and Q_k is the chiral order parameter defined in the plaquette D_k. The second terms introduced in the eq.(3.2) are the effective interaction which represent the most relevant effect of the outside of the cluster which induces the chiral order.

We put the following self-consistency condition[4]

$$\langle Q_0 \rangle = \langle Q_l \rangle \qquad \text{for all} \quad l \in \partial\Omega \tag{3.3}$$

to determine the super-effective-fields $\{\Lambda_k\}$, where the brackets denote the thermal average for $\mathcal{H}_{eff}$:

$$\langle A \rangle = \mathrm{Tr} A \exp(-\beta\mathcal{H}_{eff}) / \mathrm{Tr} \exp(-\beta\mathcal{H}_{eff}). \tag{3.4}$$

When $T > T_c$, eq.(3.3) has only trivial solutions $\{\Lambda_k = 0\}$, whereas for $T < T_c$, it has non-trivial solutions $\{\Lambda_k\}$. The emergence of non-zero solutions $\{\Lambda_k\}$ means the breakdown of symmetry of the original Hamiltonian $\mathcal{H}$ and the corresponding

$\langle Q_0\rangle_\Lambda$ is no longer equal to zero. We assume that the phase transition is of second order and therefore $\{\Lambda_k\}$ are small near $T = T_c$. Expanding eq.(3.3) with respect to Λ_k, we obtain[4]

$$\sum_{k\in\partial\Omega}\{\langle Q_0; Q_k\rangle_\Omega - \langle Q_l; Q_k\rangle_\Omega\}\lambda_k = 0 \tag{3.5}$$

for l=1,2,...,z, where $\lambda_k \equiv \beta\Lambda_k$, and $\langle A; B\rangle_\Omega$ denotes Kubo's canonical correlation:

$$\langle A; B\rangle_\Omega = \frac{1}{\beta}\int_0^\beta \langle AB(i\hbar\lambda)\rangle_\Omega d\lambda \tag{3.6}$$

$$B(z) = \exp(iz\mathcal{H}_\Omega)B\exp(-iz\mathcal{H}_\Omega). \tag{3.7}$$

Here $\langle\ldots\rangle_\Omega$ denotes the thermal average for the cluster Hamiltonian $\mathcal{H}_\Omega$. We have used the fact that $\langle Q_j\rangle_\Omega = 0$ because of the symmetry of $\mathcal{H}_\Omega$.

The critical point T_c in this approximation is determined from the zero of the determinant of eq.(3.5). If the relevant cluster is isotropic, eq.(3.5) to determine T_c is reduced[4] to

$$f(T_c) = 0 \quad ; \quad f(T) \equiv \sum_{k\in\partial\Omega}\langle Q_0; Q_k\rangle_\Omega - \langle Q_l; Q_k\rangle_\Omega \tag{3.8}$$

because of the symmetry of the cluster.

We see also that the corresponding susceptibility χ_Q diverges at $T = T_c$. We consider[4] the Hamiltonian

$$\mathcal{H} = \mathcal{H}_\Omega - \sum_{k\in\partial\Omega}\Lambda_k Q_k - H\sum_{j\in\Omega} Q_j, \tag{3.9}$$

where H is a uniform field conjugate to the chiral order Q. The susceptibility χ_Q is given[4] by

$$\chi_Q \equiv \left.\frac{\partial}{\partial H}\langle Q\rangle\right|_{H=0}$$

$$= \beta\Big(\sum_{j\in\Omega}\langle Q_0; Q_j\rangle_\Omega + \sum_{k\in\partial\Omega} x_k\langle Q_0; Q_k\rangle_\Omega\Big) \tag{3.10}$$

where

$$x_k \equiv \left.\frac{\partial\Lambda_k}{\partial H}\right|_{H=0}, \tag{3.11}$$

and the self-consistency condition at $T > T_c$ becomes[4]

$$\sum_{k\in\partial\Omega}(\langle Q_0; Q_k\rangle_\Omega - \langle Q_l; Q_k\rangle_\Omega)x_k = \sum_{j\in\Omega}(\langle Q_l; Q_j\rangle_\Omega - \langle Q_0; Q_j\rangle_\Omega) \tag{3.12}$$

up to the first order of H and λ. If we write the eq.(3.12) as $F_{lk}x_k = h_l$ where

$$F_{ij} \equiv \langle Q_0; Q_j\rangle_\Omega - \langle Q_i; Q_j\rangle_\Omega \tag{3.13}$$

$$h_i \equiv \sum_{k\in\Omega}\langle Q_i; Q_k\rangle_\Omega - \langle Q_0; Q_k\rangle_\Omega \tag{3.14}$$

$$i, j \in \partial\Omega \quad , \quad k \in \Omega, \tag{3.15}$$

the susceptibility χ_Q is expressed[4] as

$$\chi_Q = \beta(\sum_{j\in\Omega}\langle Q_0; Q_j\rangle_\Omega + \sum_{k,l\in\partial\Omega} F^{-1}_{kl} h_l \langle Q_0; Q_k\rangle_\Omega). \tag{3.16}$$

Thus the susceptibility χ_Q diverges at $\det(F_{ij}) = 0$.

We can easily construct the systematic series of approximations by enlarging the cluster Ω. By applying the CAM analysis[7,8] to the series of approximations, we can obtain information about the true critical temperatures T_c^* and the relevant exponents.

3.2 Bethe-like approximation

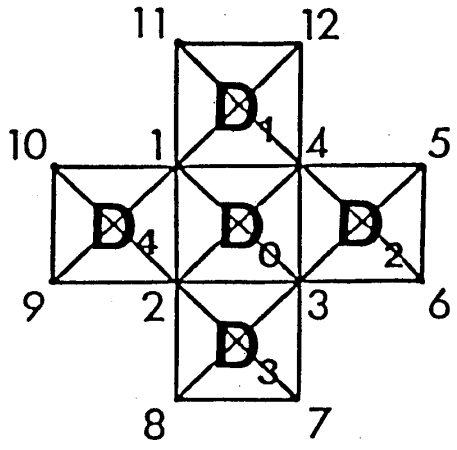

Fig. 1.4: The cluster of the Bethe approximation.

The cluster we consider is shown in the Fig.1.4. In this case, the equation to determine T_c is given by eq.(3.8) and the susceptibility χ_Q is explicitly given[4] by

$$\chi_Q = \beta(\sum_{j\in\Omega}\langle Q_0; Q_j\rangle_\Omega + \sum_{l\in\partial\Omega} \frac{\sum_{j\in\Omega}\langle Q_l; Q_j\rangle_\Omega - \langle Q_0; Q_j\rangle}{\sum_{k\in\partial\Omega}\langle Q_0; Q_k\rangle_\Omega - \langle Q_l; Q_k\rangle_\Omega}\langle Q_0; Q_l\rangle_\Omega) \tag{3.17}$$

Now if we make a further approximation[4], namely the "Kirkwood" approximation :

$$\langle Q_i; Q_j\rangle_\Omega \simeq \langle Q_i; Q_0\rangle_\Omega \langle Q_0; Q_j\rangle_\Omega / \langle Q_0; Q_0\rangle_\Omega \tag{3.18}$$

for $i \neq j \in \partial\Omega$ and

$$\langle Q_0; Q_0\rangle_\Omega \simeq \langle Q_l; Q_l\rangle_\Omega, \quad \text{for} \quad l \in \partial\Omega, \tag{3.19}$$

then we obtain[4] the following expression of the susceptibility χ_Q:

$$\chi_Q = \beta \frac{\langle Q_0; Q_0\rangle_\Omega(\langle Q_0; Q_0\rangle_\Omega + \langle Q_0; Q_l\rangle_\Omega)}{\langle Q_0; Q_0\rangle_\Omega - (z-1)\langle Q_0; Q_l\rangle_\Omega} \tag{3.20}$$

where $l \in \partial\Omega$. Therefore the equation to determine T_c is reduced[4] to

$$\mathcal{F}_c(T_c) = 1 \quad ; \quad \mathcal{F}_c(T) \equiv \frac{(z-1)\langle Q_0; Q_l\rangle_\Omega}{\langle Q_0; Q_0\rangle_\Omega}. \tag{3.21}$$

Here z denotes the number of nearest neighbors. The quantity $\mathcal{F}_c(T)$ is a normalized canonical correlation function. Physically it describes the tendency to order or cooperate. At high temperatures, the correlation $\langle Q_0; Q_l\rangle_\Omega$ is considered to be small compared with the auto-correlation $\langle Q_0; Q_0\rangle_\Omega$, namely $\mathcal{F}_c \ll 1$. As the temperature decreases, the correlation $\langle Q_0; Q_l\rangle_\Omega$ increases and at the critical temperature T_c, the function $\mathcal{F}_c$ passes through $\mathcal{F}_c = 1$.

Next let us consider the limit $T \to 0$. In this limit we find that the canonical correlations $\langle Q_i; Q_j\rangle_\Omega$ goes to zero for finite quantum systems. The canonical correlations at $T = 0$ are given by[4]

$$\lim_{T\to 0}\langle A; B\rangle \equiv \langle A; B\rangle_g = \frac{1}{N_g}\sum_{k=1}^{N_g}\sum_{l=1}^{N_g}\langle\Phi_k|A|\Phi_l\rangle\langle\Phi_l|B|\Phi_k\rangle \tag{3.22}$$

where Φ_k denotes the k-th ground state and N_g denotes the degeneracy of the ground states. In the case of finite quantum systems, the ground state is usually non-degenerate and symmetric. Therefore if the operators A and B violate the symmetry of the original Hamiltonian, we have[4]

$$\lim_{T\to 0}\langle A; B\rangle_\Omega = \langle A\rangle_g\langle B\rangle_g = 0 \tag{3.23}$$

where $\langle\cdots\rangle_g$ denotes the expectation value for the ground state. The normalized correlation functions have finite values at $T = 0$, because the numerator and the denominator go to zero in the same order as $T \to 0$.

Thus $\mathcal{F}_c(T)$ is an almost monotonically decreasing function of T , and the above physical interpretation of $\mathcal{F}_c(T)$ is justified. We can study a possibility of the phase transition by investigating the T-dependence of $\mathcal{F}_c(T)$.

We can also consider the direct correlation $\langle AB\rangle$ instead of the canonical correlation $\langle A; B\rangle$. It is based on the decoupled density-matrix formalism[4]. In this case, the equation to determine T_c becomes

$$f(T_c)_d = 0 \quad ; \quad f(T)_d \equiv \sum_{k\in\partial\Omega}\langle Q_0 Q_k\rangle_\Omega - \langle Q_l Q_k\rangle_\Omega, \tag{3.24}$$

and if we make the "Kirkwood" approximation we get[4]

$$\mathcal{F}_d(T) = \frac{(z-1)\langle Q_0 Q_l\rangle_\Omega}{\langle Q_0 Q_0\rangle_\Omega}. \tag{3.25}$$

The threshold is also given by $\mathcal{F}_d = 1$. In most cases, $\mathcal{F}_d$ is larger than $\mathcal{F}_c$. At high temperatures direct correlations coincide with canonical correlations, however at $T \longrightarrow 0$ they are different because the direct correlation remains finite if the product of two operators does not violate the symmetry of the original Hamiltonian.

Anyway, in the SEFT formulation, we can study a possibility of phase transitions from the behavior of the normalized correlation function $\mathcal{F}_c(T)$ or $\mathcal{F}_d(T)$ evaluated in finite clusters.

4 Numerical Calculations

4.1 4-Spin Cluster Approximation

First we consider the 4-spin cluster shown in the Fig. 1.8.(a) to determine how to choose the order parameter Q defined on the square plaquette. The Hamiltonian is given by

$$\mathcal{H}_\Omega = J(\boldsymbol{S}_1\cdot\boldsymbol{S}_2 + \boldsymbol{S}_2\cdot\boldsymbol{S}_3 + \boldsymbol{S}_3\cdot\boldsymbol{S}_4 + \boldsymbol{S}_4\cdot\boldsymbol{S}_1) + J'(\boldsymbol{S}_1\cdot\boldsymbol{S}_3 + \boldsymbol{S}_2\cdot\boldsymbol{S}_4) \tag{4.1}$$

where $J > 0$ and $J' > 0$. The important parameter is the ratio of the nearest neighbor interaction J and the next nearest neighbor interaction J'. Thus we take $J = 1$ and $t \equiv J'/J$ through out this section. Then $\mathcal{H}_\Omega$ is written as

$$\mathcal{H}_\Omega = (\boldsymbol{S}_1\cdot\boldsymbol{S}_2 + \boldsymbol{S}_2\cdot\boldsymbol{S}_3 + \boldsymbol{S}_3\cdot\boldsymbol{S}_4 + \boldsymbol{S}_4\cdot\boldsymbol{S}_1) + t(\boldsymbol{S}_1\cdot\boldsymbol{S}_3 + \boldsymbol{S}_2\cdot\boldsymbol{S}_4). \tag{4.2}$$

We calculated the correlations of the chiral operators $\{X_{ijk}\}$ in the plaquette. We obtain

$$\langle X_{123}; X_{234}\rangle_\Omega < 0 \tag{4.3}$$

$$\langle X_{123}; X_{341}\rangle_\Omega > 0 \tag{4.4}$$

for any T. The above inequalities hold even in the case of direct correlations as is shown in Appendix C. We choose the order parameter Q_{1234} on the plaquette(1234) as

$$Q_{1234} \equiv X_{123} - X_{234} + X_{341} - X_{412}. \tag{4.5}$$

Here Q_{1234} is different from the difference $(Pl_{1234} - Pl_{1432})$, because the sign of X_{412} is negative. The physical meaning of Q_{1234} in the fermionic representation is not clear, but to avoid the cancellation of X's in the plaquette we adopt this order

#	Eigenvalues of $\mathcal{H}_\Omega$	Eigenstates of $\mathcal{H}_\Omega$
1	$t/2+1$	$\|\uparrow\uparrow\uparrow\uparrow\rangle$
2	$t/2+1$	$1/2\{\|1\rangle+\|2\rangle+\|3\rangle+\|4\rangle\}$
3	$-t/2$	$1/2\{\|1\rangle+i\|2\rangle+i^2\|3\rangle+i^3\|4\rangle\}$
4	$t/2-1$	$1/2\{\|1\rangle+i^2\|2\rangle+\|3\rangle+i^2\|4\rangle\}$
5	$-t/2$	$1/2\{\|1\rangle+i^3\|2\rangle+i^2\|3\rangle+i\|4\rangle\}$
6	$t/2-2$	$1/\sqrt{3}\{1/2[\|12\rangle+\|23\rangle+\|34\rangle+\|41\rangle]-[\|13\rangle+\|24\rangle]\}$
7	$t/2+1$	$1/\sqrt{6}\{\|12\rangle+\|23\rangle+\|34\rangle+\|41\rangle+\|24\rangle+\|13\rangle\}$
8	$-t/2$	$1/2\{\|12\rangle+i\|23\rangle+i^2\|34\rangle+i^3\|41\rangle\}$
9	$-3t/2$	$1/2\{\|12\rangle+i^2\|23\rangle+\|34\rangle+i^2\|41\rangle\}$
10	$-t/2$	$1/2\{\|12\rangle+i^3\|23\rangle+i^2\|34\rangle+i\|41\rangle\}$
11	$t/2-1$	$1/2\{\|13\rangle-\|24\rangle$
12	$t/2+1$	$1/2\{\|1\rangle'+\|2\rangle'+\|3\rangle'+\|4\rangle'\}$
13	$-t/2$	$1/2\{\|1\rangle'+i\|2\rangle'+i^2\|3\rangle'+i^3\|4\rangle'\}$
14	$t/2-1$	$1/2\{\|1\rangle'+i^2\|2\rangle'+\|3\rangle'+i^2\|4\rangle'\}$
15	$-t/2$	$1/2\{\|1\rangle'+i^3\|2\rangle'+i^2\|3\rangle'+i\|4\rangle'\}$
16	$t/2+1$	$\|\downarrow\downarrow\downarrow\downarrow\rangle$

Table I.1: Here $i^2=-1$, the numbers in the kets $|\cdots\rangle$ denote the sites of down spins and the numbers in the kets $|\cdots\rangle'$ denote the sites of up spins, e. g. ,$|4\rangle'=|123\rangle$.

parameter Q_{1234}. In the case of the Hubbard model or t-J model, we have to choose $Pl_{1234}-Pl_{1432}$ as an order parameter, for its physical meaning is clear.

We can explicitly write down the eigenstates and the eigenvalues of the Hamiltonian(4.2) as in the table I.1. In the following we denote the state $|\uparrow\uparrow\downarrow\downarrow\rangle$ by $|34\rangle$; the numbers in the kets $|\cdots\rangle$ denote the sites of down spins. The ground state is $(1/\sqrt{3})\{1/2[|12\rangle+|23\rangle+|34\rangle+|41\rangle]-[|13\rangle+|24\rangle]\}$ with the ground state energy $t/2-2$ for $1\geq t\geq 0$. This ground state is a total spin $S=0$ state and symmetric. Therefore the expectation value of X_{123} for this ground state vanishes ;

$$\langle \text{Ground State}|X_{123}|\text{Ground State}\rangle = 0. \tag{4.6}$$

From the table I.1, we see that when $t=1$ another total spin $S=0$ state $(1/2)\{|12\rangle-|23\rangle+|34\rangle-|41\rangle\}$ is also the ground state. Thus at $t=1$ the ground states are degenerate. They are written as the linear combinations of two spin singlet states $|S=0\rangle^+$ and $|S=0\rangle^-$, which are defined previously. We can easily find that

$$\frac{1}{\sqrt{3}}\{\frac{1}{2}[|12\rangle+|23\rangle+|34\rangle+|41\rangle]-[|13\rangle+|24\rangle]\} = |A\rangle+\sqrt{3}i|B\rangle \tag{4.7}$$

$$\frac{1}{2}\{|12\rangle-|23\rangle+|34\rangle-|41\rangle\} = |A\rangle-\frac{i}{\sqrt{3}}|B\rangle \tag{4.8}$$

where

$$|A\rangle \equiv \frac{1}{\sqrt{2}}\{|S=0\rangle^{+}+|S=0\rangle^{-}\}$$
$$= \frac{1}{\sqrt{3}}\{|34\rangle+|12\rangle-\frac{1}{2}[|24\rangle+|14\rangle+|23\rangle+|13\rangle]\} \quad (4.9)$$
$$|B\rangle \equiv \frac{1}{\sqrt{2}}\{|S=0\rangle^{+}-|S=0\rangle^{-}\}$$
$$= \frac{i}{2}\{[|24\rangle+|13\rangle]-[|14\rangle+|23\rangle]\} \quad (4.10)$$

and

$$|S=0\rangle^{+} = |34\rangle+|12\rangle+\omega|24\rangle+\omega|13\rangle+\omega^{2}|14\rangle+\omega^{2}|23\rangle \quad (4.11)$$
$$|S=0\rangle^{-} = |34\rangle+|12\rangle+\omega^{2}|24\rangle+\omega^{2}|13\rangle+\omega|14\rangle+\omega|23\rangle. \quad (4.12)$$

Here ω denotes the cube root of unity. Therefore the ground state for $t \neq 1$ is the superposition of the states $|S=0\rangle^{+}$ and $|S=0\rangle^{-}$, which are eigenstates of X_{123}, with equal weight. Only at $t=1$ another state, which is also the superposition of $|S=0\rangle^{+}$ and $|S=0\rangle^{-}$, has the same energy. Thus each of the eigenstates of X_{123} can be the ground states at $t=1$.

Now let us consider the behavior of normalized correlation functions.

a) Direct correlations

We define the normalized direct correlation functions $\mathcal{F}_d^1$ and $\mathcal{F}_d^2$ as follows

$$\mathcal{F}_d^1(T) \equiv \langle X_{123}X_{234}\rangle_\Omega / \langle X_{123}^2\rangle_\Omega \quad (4.13)$$
$$\text{and} \quad \mathcal{F}_d^2(T) \equiv \langle X_{123}X_{341}\rangle_\Omega / \langle X_{123}^2\rangle_\Omega. \quad (4.14)$$

Note that $|\mathcal{F}_d^1|$ and $|\mathcal{F}_d^2|$ are monotonically decreasing functions of T and that

$$\mathcal{F}_d^1(0)=-1 \quad \mathcal{F}_d^1(\infty)=0$$
$$\mathcal{F}_d^2(0)=1 \quad \mathcal{F}_d^2(\infty)=0. \quad (4.15)$$

The exact expressions of the direct correlations are given in Appendix C. In the case of the vector chiral order, the correlation at the high temperature limit remains non-vanishing, if the two chiral operators share the same bond, but in the case of the scalar chiral order the correlation goes to zero even if the two chiral operators share the same bond.

b) Canonical correlations

In the same way, the normalized canonical correlations $\mathcal{F}_c^1$ and $\mathcal{F}_c^2$ are defined as follows:

$$\mathcal{F}_c^1(T) \equiv \langle X_{123}; X_{234}\rangle_\Omega / \langle X_{123}; X_{123}\rangle_\Omega \tag{4.16}$$

$$\text{and} \quad \mathcal{F}_c^2(T) \equiv \langle X_{123}; X_{341}\rangle_\Omega / \langle X_{123}; X_{123}\rangle_\Omega. \tag{4.17}$$

The behavior of the normalized canonical correlations is almost the same as that of the direct correlations as follows:

$$\begin{aligned} \mathcal{F}_d^1(0) = -1 \qquad & \mathcal{F}_d^1(\infty) = 0 \\ \mathcal{F}_d^2(0) = 1 \qquad & \mathcal{F}_d^2(\infty) = 0. \end{aligned} \tag{4.18}$$

However, bare canonical correlations behave quite differently near $T = 0$. For $0 \leq t < 1$, we have

$$\langle X_{ijk}; X_{lmn}\rangle_\Omega \to 0 \quad \text{as} \quad T \to 0 \tag{4.19}$$

but for $t = 1$, the canonical correlation $\langle X; X\rangle_\Omega$ goes to a non-zero value at $T = 0$, because X commutes with the Hamiltonian (4.2) and the ground states are degenerate. In fact, we have

$$\begin{aligned} \langle X; X\rangle_g &= ({}^\alpha\langle S = 0|X|S = 0\rangle^\alpha)^2 \\ &= (\frac{\sqrt{3}}{4})^2 = \frac{3}{16}. \end{aligned} \tag{4.20}$$

The behavior of the canonical correlations at $t = 1$ and $t = 1/2$ are shown in the Fig. 1.5 and Fig. 1.6. It is quite interesting that the normalized canonical correlation shows almost the same behavior at $t = 1$ and $t = 1/2$, though the bare canonical correlation behaves differently near $T = 0$.

4.2 6-Spin Cluster Approximation

Next we consider the cluster of six spins shown in the Fig. 1.8.(b). We calculate the correlations between the chiral orders $\{Q_{ijkl}\}$ defined on the square plaquette(ijkl). The Hamiltonian is

$$\begin{aligned} \mathcal{H}_\Omega &= (\boldsymbol{S}_1 \cdot \boldsymbol{S}_2 + \boldsymbol{S}_2 \cdot \boldsymbol{S}_3 + \boldsymbol{S}_3 \cdot \boldsymbol{S}_4 + \boldsymbol{S}_1 \cdot \boldsymbol{S}_4 + \boldsymbol{S}_4 \cdot \boldsymbol{S}_5 + \boldsymbol{S}_5 \cdot \boldsymbol{S}_6 + \boldsymbol{S}_6 \cdot \boldsymbol{S}_3) \\ &\quad + t(\boldsymbol{S}_1 \cdot \boldsymbol{S}_3 + \boldsymbol{S}_2 \cdot \boldsymbol{S}_4 + \boldsymbol{S}_4 \cdot \boldsymbol{S}_6 + \boldsymbol{S}_3 \cdot \boldsymbol{S}_5). \end{aligned} \tag{4.21}$$

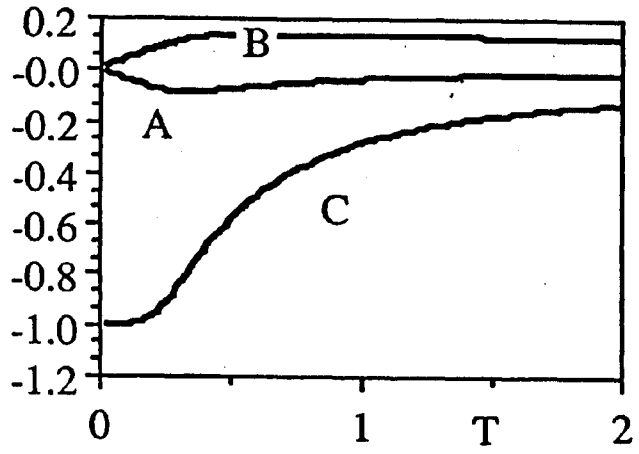

Fig. 1.5: Temperature-dependence of canonical correlations of 4-Spin System at $J'/J = 1/2$. Curve A denotes $\langle X_{123}; X_{234}\rangle_\Omega$, Curve B denotes $\langle X_{123}; X_{123}\rangle_\Omega$ and Curve C denotes $\mathcal{F}_c^1(T) = \langle X_{123}; X_{234}\rangle_\Omega / \langle X_{123}; X_{123}\rangle_\Omega$.

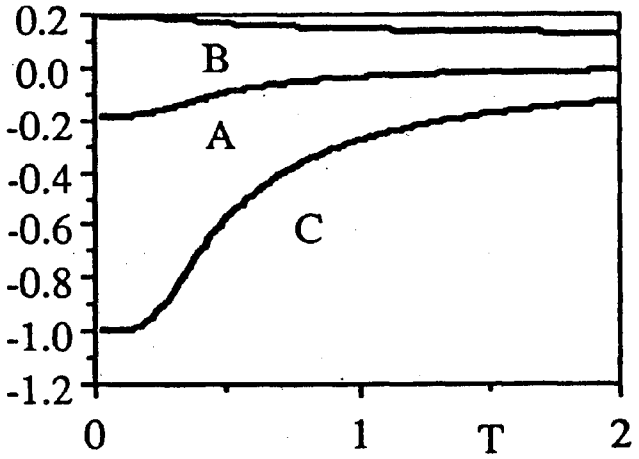

Fig. 1.6: Temperature-dependence of canonical correlations of 4-Spin System at $J'/J = 1$. Curve A denotes $\langle X_{123}; X_{234}\rangle_\Omega$, Curve B denotes $\langle X_{123}; X_{123}\rangle_\Omega$ and Curve C denotes $\mathcal{F}_c^1(T) = \langle X_{123}; X_{234}\rangle_\Omega / \langle X_{123}; X_{123}\rangle_\Omega$.

a) Direct correlations

The normalized correlation function is given as

$$\mathcal{F}_d(T) \equiv (z-1)\frac{\langle Q_{1234} Q_{4365}\rangle_\Omega}{\langle Q_{1234}^2\rangle_\Omega} \tag{4.22}$$

where z is the number of nearest neighbors and in the present case $z = 4$. The behaviors of $\mathcal{F}_d(T)$ at $t = 0.1, 0.5, 0.9$ are shown in the Fig. 1.7. In each case we obtain $\mathcal{F}_d < 1$ and consequently there is no critical point T_c. Furthermore the tendency to ordering is suppressed by enlarging the parameter t ; by the introduction of frustrations.

b) Canonical correlations

In the case of the canonical correlation :

$$\mathcal{F}_c(T) \equiv (z-1)\frac{\langle Q_{1234}; Q_{4365}\rangle_\Omega}{\langle Q_{1234}; Q_{1234}\rangle_\Omega}, \tag{4.23}$$

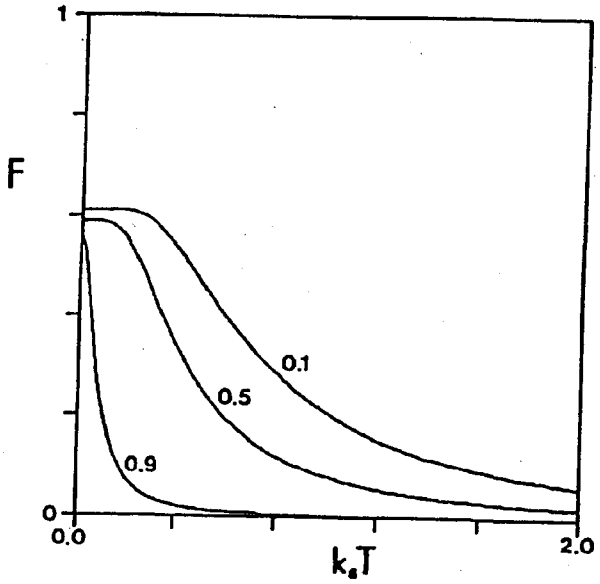

Fig. 1.7: $\mathcal{F}_d(T)$ of 6-Spin Cluster for $J'/J = 0.1, 0.5, 0.9$.

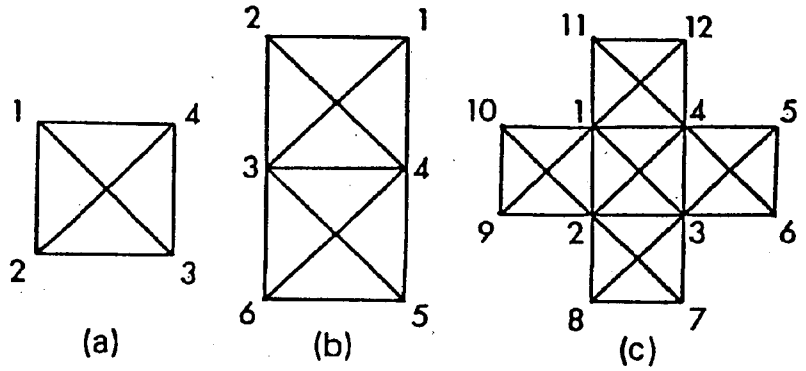

Fig. 1.8: Clusters we consider.

the result is shown in the Figs.1.9–1.12. The quantity $\mathcal{F}_c$ is much smaller than $\mathcal{F}_d$. Thus there is no critical point T_c. The t-dependence of the tendency to ordering is the same as that of the direct correlations. In the present case, the order parameter Q does not commute with $\mathcal{H}_\Omega$ for any t, so that the bare canonical correlations go to zero as $T \to 0$.

4.3 12-Spin Cluster Approximation

We consider the 12-spin cluster shown in the Fig.1.8.(c). The Hamiltonian is

$$\mathcal{H}_\Omega = \sum_{n.n.} \boldsymbol{S}_i \cdot \boldsymbol{S}_j + \sum_{n.n.n.} \boldsymbol{S}_i \cdot \boldsymbol{S}_j. \tag{4.24}$$

a) Direct correlations

The T-dependence of the normalized correlation function defined by

$$\mathcal{F}_d(T) = (z-1)\frac{\langle Q_{1234} Q_{4365} \rangle_\Omega}{\langle Q_{1234}^2 \rangle_\Omega} \tag{4.25}$$

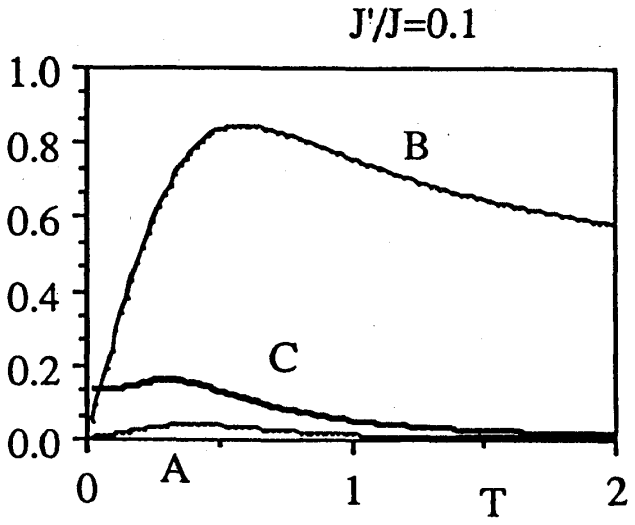

Fig. 1.9: Temperature-dependence of canonical correlations of 6-Spin Cluster at $J'/J = 0.1$. Curve A denotes $\langle Q_{1234}; Q_{4365}\rangle_\Omega$, Curve B denotes $\langle Q_{1234}; Q_{1234}\rangle_\Omega$ and Curve C denotes $\mathcal{F}_c(T) = 3 \cdot \langle Q_{1234}; Q_{4365}\rangle_\Omega / \langle Q_{1234}; Q_{1234}\rangle_\Omega$.

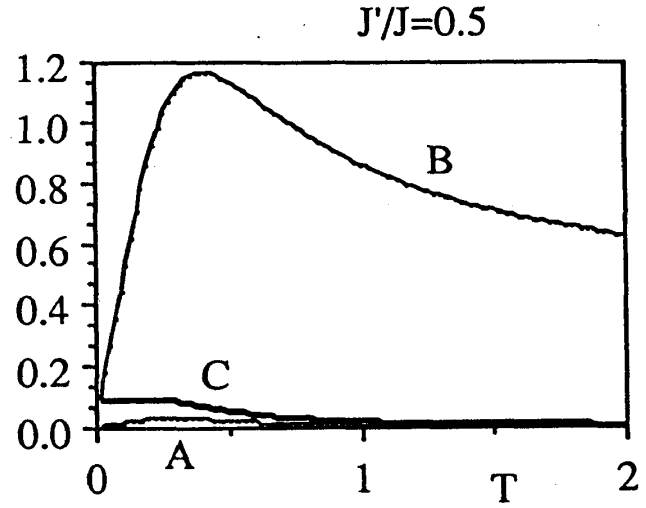

Fig. 1.10: Temperature-dependence of canonical correlations of 6-Spin Cluster at $J'/J = 0.5$. Curve A denotes $\langle Q_{1234}; Q_{4365}\rangle_\Omega$, Curve B denotes $\langle Q_{1234}; Q_{1234}\rangle_\Omega$ and Curve C denotes $\mathcal{F}_c(T) = 3 \cdot \langle Q_{1234}; Q_{4365}\rangle_\Omega / \langle Q_{1234}; Q_{1234}\rangle_\Omega$.

is shown in the Fig. 1.13 and Fig. 1.14. The behavior is almost the same as that of the 6-spin cluster and we have $\mathcal{F}_d(T) < 1$ for any T. We also investigate the T-dependence of $f(T)_d$ without making the "Kirkwood" approximation. Our result is shown in the Fig. 1.15. The T-dependence of $f(T)_d$ is interpreted as follows. By definition, we have

$$f(T)_d = \sum_{k\in\partial\Omega} \langle Q_0; Q_k\rangle_\Omega - \langle Q_l; Q_k\rangle_\Omega \tag{4.26}$$

$$= 4\langle Q_{1,2,3,4}Q_{4,3,6,5}\rangle_\Omega - 2\langle Q_{11,1,4,12}Q_{4,3,6,5}\rangle_\Omega - \langle Q_{10,9,2,1}Q_{4,3,6,5}\rangle_\Omega - \langle Q_{4,3,6,5}Q_{4,3,6,5}\rangle_\Omega \tag{4.27}$$

and T_c is determined from the condition that $f(T_c)_d = 0$. The right hand side of eq.(4.26) involves the auto-correlation $-\langle Q_l; Q_l\rangle_\Omega$. Thus at high temperatures f_d is negative. As the temperature decreases, other correlations increase, and consequently the critical point T_c is obtained as the point where the boundary to boundary correlations are equal to the center to boundary correlations. However, our result shows that $f(T)_d <$

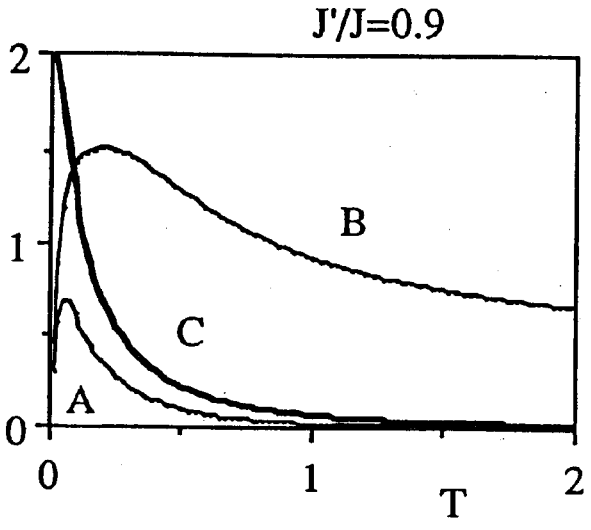

Fig. 1.11: Temperature-dependence of canonical correlations of 6-Spin Cluster at $J'/J = 0.9$. Curve A denotes $\langle Q_{1234}; Q_{4365}\rangle_\Omega \cdot 10^2$, Curve B denotes $\langle Q_{1234}; Q_{1234}\rangle_\Omega$ and Curve C denotes $\mathcal{F}_c(T) \cdot 10^2 = 3 \cdot (\langle Q_{1234}; Q_{4365}\rangle_\Omega / \langle Q_{1234}; Q_{1234}\rangle_\Omega) \cdot 10^2$.

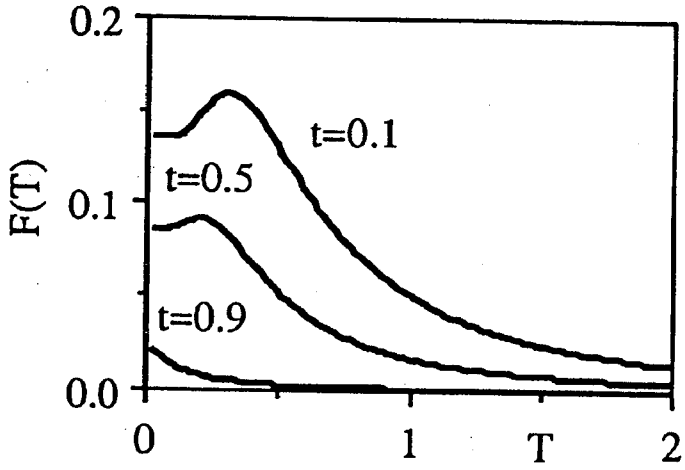

Fig. 1.12: $\mathcal{F}_c(T)$ of 6-Spin Cluster at $J'/J = 0.1, 0.5, 0.9$.

0 for any T as in the Fig. 1.15. Thus, we arrive finally at the conclusion that there exists no T_c even in the 12-spin cluster approximation.

5 Discussion

We have calculated the normalized correlations of the scalar chiral orders in the small lattices. In the 6-spin cluster and 12-spin cluster approximations we have obtained no critical temperature T_c. The correlations between the scalar chiral orders are too small and the tendency to order is suppressed by the introduction of frustrations. Thus from our calculations we get no indication of the existence of the scalar chiral order in the two-dimensional spin 1/2 Heisenberg model with n.n.n. interactions. However, our clusters used here are small and calculations for larger clusters are needed to get more reliable results.

Classically this model has two phases. When $0 < t < 1/2$ the ground state is the

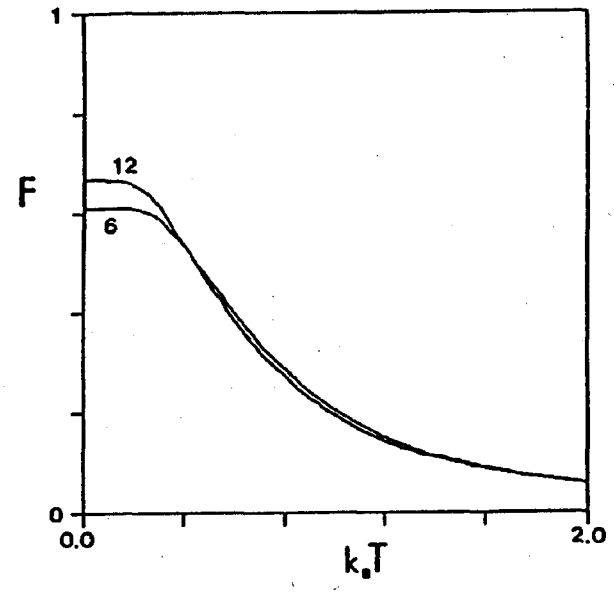

Fig. 1.13: $\mathcal{F}_d(T)$ of 6-Spin Cluster and 12-Spin Cluster at $J'/J = 0.1$.

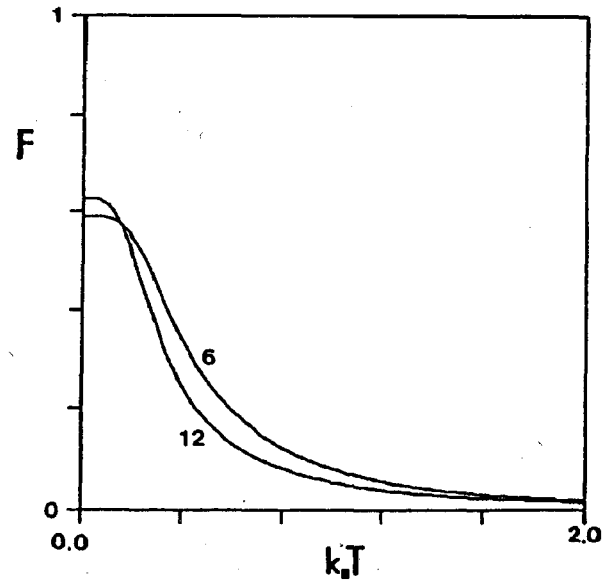

Fig. 1.14: $\mathcal{F}_d(T)$ of 6-Spin Cluster and 12-Spin Cluster at $J'/J = 0.5$.

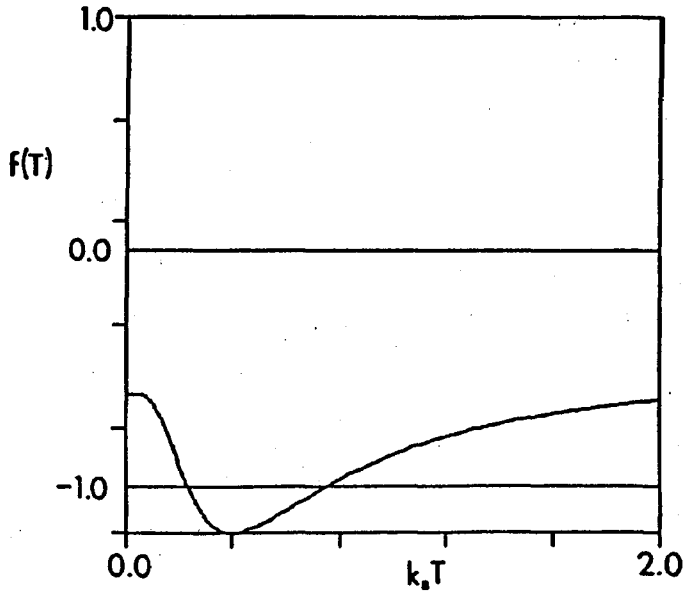

Fig. 1.15: $f_d(T)$ of 12-Spin Cluster at $J'/J = 0.5$.

Néel state. But when $t \geq 1/2$ the ground state decouples into the two Néel sublattices with an energy independent of the angle between the corresponding staggered magnetizations. Thus the ground states for $t > 1/2$ are highly degenerate. Therefore we expect that the drastic change of the property of the ground state at $t = 1/2$ also occurs in quantum systems. In our calculations, however, there occurs no expected change at $t = 1/2$. This seems to be caused owing to the smallness of our clusters. In the clusters we consider here, the number of the nearest neighbor interactions is larger than that of the next nearest neighbor ones because of the boundary effect, so that the influence of the n.n.n. interactions is suppressed. In a system of 20 spins, the change of the ground state property at $t \approx 0.6$ has been reported[11]. The property of the ground state is important but at finite temperatures the orders in the ground state are often destroyed by thermal fluctuations especially in two dimensional systems.

Thus ,to know what really happens in quantum spin systems in the thermodynamic limit, we have to investigate larger systems not only at $T = 0$ but also at finite temperatures.

Chapter II

Vector Chiral Order

1 Introduction

It is proved using Bogoliubov's inequality that no vector chiral order appears at finite temperatures in the two-dimensional antiferromagnetic Heisenberg model with short-range interaction.

In this chapter, we discuss the vector chiral order defined by $\boldsymbol{Q}_{i,j,k} \propto (\boldsymbol{S}_i \times \boldsymbol{S}_j + \boldsymbol{S}_j \times \boldsymbol{S}_k + \boldsymbol{S}_k \times \boldsymbol{S}_i)$ at the three lattice points i, j and k, while the scalar chiral order is defined by $X_{i,j,k} = \boldsymbol{S}_i \cdot (\boldsymbol{S}_j \times \boldsymbol{S}_k)$.

Since Villain[12] pointed out two-fold degeneracy in fully frustrated spin systems, there have been reported many numerical calculations and approximate theories[12-20,4,5] about the vector chiral order in frustrated spin systems. Especially in quantum spin systems, Fujiki and Betts[17,18] and Nishimori and Nakanishi[19] have investigated the ground state of the antiferromagnetic X–Y model and Heisenberg model on the triangular lattice by exact diagonalization. Matsubara and Inawashiro[20] studied the antiferromagnetic X–Y model on the triangular lattice at finite temperatures by using a Monte Carlo method.

Their calculations suggest that there is no vector chiral order in the Heisenberg model.

2 Absence of the Vector Chiral Order in the Two-Dimensional Heisenberg Model

We consider here the two-dimensional square lattice and triangular lattice. For quantum spin systems, the normalized chirality operator

$$Q_{i,j,k} = \frac{2\sqrt{3}}{3}(\boldsymbol{S}_i \times \boldsymbol{S}_j + \boldsymbol{S}_j \times \boldsymbol{S}_k + \boldsymbol{S}_k \times \boldsymbol{S}_i) \tag{2.1}$$

is defined[17,18] in each plaquette on the triangular lattice, following definitions for classical spins[12-16]. We consider the z-component of this operator and define a chiral order parameter for each lattice as follows.

i)For the square lattice, the total chiral order $\tilde{Q}_{sq}$ is defined by

$$\tilde{Q}_{sq} \equiv \sum_i \varepsilon_i Q_i^z \quad ; \quad \varepsilon_i = \exp(i\boldsymbol{\kappa}\cdot\boldsymbol{r}_i) \quad \text{and} \quad \boldsymbol{\kappa} = (\pi,\pi) \tag{2.2}$$

where ε_i is a modular factor and Q_i^z is the z-component of the chirality operator defined on the plaquette shown in the Fig.2.1. It is explicitly given by

$$\begin{aligned} Q_i^z &\equiv \frac{\sqrt{3}}{4}(\boldsymbol{Q}_{i,i+u,i+u+v} + \boldsymbol{Q}_{i+u,i+u+v,i+v} + \boldsymbol{Q}_{i+u+v,i+v,i} + \boldsymbol{Q}_{i+v,i,i+u})^z \\ &= (\boldsymbol{S}_i \times \boldsymbol{S}_{i+u} + \boldsymbol{S}_{i+u} \times \boldsymbol{S}_{i+u+v} + \boldsymbol{S}_{i+u+v} \times \boldsymbol{S}_{i+v} + \boldsymbol{S}_{i+v} \times \boldsymbol{S}_i)^z, \end{aligned} \tag{2.3}$$

where $u(v)$ is a unit vector of the $x(y)$-direction and $\boldsymbol{r}_i$ is the position vector of the site i. Lattice spacing is taken as a unit length.

ii)For the triangular lattice, we have

$$\tilde{Q}_{tr} \equiv \frac{\sqrt{3}}{2}\sum_i (\boldsymbol{Q}_{i,i+a,i+a+b} - \boldsymbol{Q}_{i,i+a+b,i+b})^z \tag{2.4}$$

where a and b denote unit vectors shown in the Fig.2.2.

The Hamiltonian to consider here is of short range. Thus we assume the Hamiltonian

$$H_0 = -\sum_{i<j} J_{ij}\boldsymbol{S}_i \cdot \boldsymbol{S}_j \tag{2.5}$$

with the couplings which satisfy the following condition.

$$J_0 \equiv \sum_j |J_{ij}||r_i - r_j|^2 < \infty \tag{2.6}$$

The present argument is similar to that of Mermin and Wagner[21]. Bogoliubov's inequality for quantum systems states that

$$\frac{1}{2}\beta\langle AA^\dagger + A^\dagger A\rangle\langle\left[[C,H],C^\dagger\right]\rangle \geq |\langle[C,A]\rangle|^2 \tag{2.7}$$

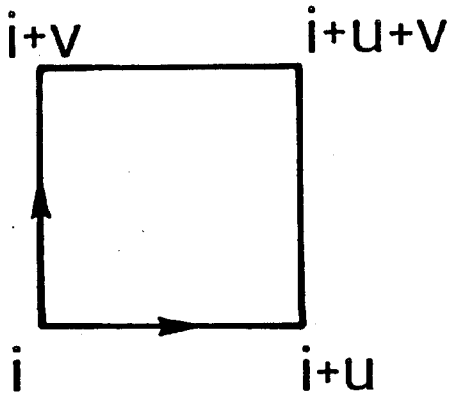

Fig. 2.1: A typical plaquette to define the chirality operator Q_i^z in the square lattice.

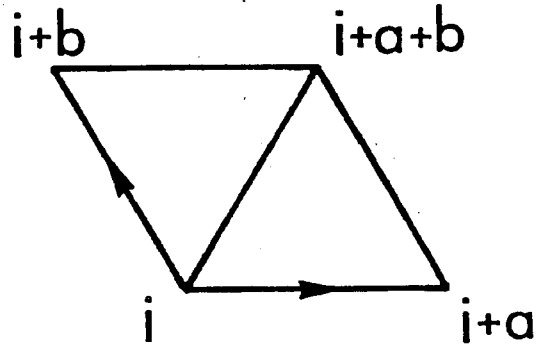

Fig. 2.2: A typical plaquette to define the combined chirality operator $\tilde{Q}_{tr}$ in the triangular lattice.

where $\beta = (k_B T)^{-1}$, H is an hermitian matrix($H = H^\dagger$), and C and A are arbitrary matrices of the same size. The angular brackets denote the following thermal average:

$$\langle B \rangle \equiv \mathrm{Tr}[B \exp(-\beta H)]/\mathrm{Tr} \exp(-\beta H) \tag{2.8}$$

and the square brackets denote a commutator.

One of the keypoints in our argument is to consider the following Hamiltonian with a super-effective field Λ[4] conjugate to the chiral order $\tilde{Q}$:

$$H = H_0 + H' \quad ; \quad H' = -\Lambda \tilde{Q}, \tag{2.9}$$

where H_0 is the Heisenberg Hamiltonian(2.5), and $\tilde{Q}$ is the chiral order parameter, given by $\tilde{Q}_{sq}(\tilde{Q}_{tr})$ in the case of the square lattice(triangular lattice).

We choose C in eq.(2.7) as

$$C(\boldsymbol{k}) = \sum_j \exp(i\boldsymbol{k} \cdot \boldsymbol{r}_j) \cdot S_j^y, \tag{2.10}$$

where $\boldsymbol{k}$ is the wave vector restricted to the first Brillouin zone. Furthermore we

choose A in eq.(2.7) as

$$A(k) = -2\sum_j \exp(-ik\cdot r_j)\cdot\varepsilon_j\cdot S_j^z\cdot[S_{j+u}^y + S_{j-u}^y - S_{j+v}^y - S_{j-v}^y] \tag{2.11}$$

in the case of the square lattice, and

$$A(k) = -2\sum_j \exp(-ik\cdot r_j)S_j^z\cdot[S_{j+a}^y - S_{j-a}^y + S_{j+b}^y - S_{j-b}^y + S_{j-a-b}^y - S_{j+a+b}^y]. \tag{2.12}$$

in the case of the triangular lattice. The direct calculation shows that

$$i[C(k), A(k)] \;=\; \tilde{Q} \tag{2.13}$$

and

$$\begin{aligned}&\left[[C(k), H], C(k)^\dagger\right]\\ &= \Lambda\tilde{Q} + 2\sum_{i<j} J_{ij}(1-\cos k\cdot(r_i - r_j))(S_i^x S_j^x + S_i^z S_j^z)\end{aligned} \tag{2.14}$$

for any k, where $\tilde{Q}$ is the chiral operator defined previously.

It follows from eq.(2.14) that

$$\langle\left[[C, H], C^\dagger\right]\rangle \le V(|\Lambda\tilde{q}| + 2J_0 s^2|k|^2) \tag{2.15}$$

where V is the volume of the system and $s^2 = S(S+1)$ and $\tilde{q} \equiv \langle\tilde{Q}\rangle/V$ is the chiral order parameter per site. Substituting eqs.(2.13) and (2.14) into Bogoliubov's inequality(2.7), and using eq.(2.15), we obtain

$$\frac{1}{2}\beta\langle A(k)A(k)^\dagger + A(k)^\dagger A(k)\rangle \;\ge\; \frac{V^2\tilde{q}^2}{V(|\Lambda\tilde{q}| + 2J_0 s^2|k|^2)} \tag{2.16}$$

Taking the summation over k's, and taking the limit $V \to \infty$, we obtain

$$\beta M \ge \int k\mathrm{d}k \frac{\tilde{q}^2}{|\Lambda\tilde{q}| + 2J_0 s^2|k|^2} \tag{2.17}$$

where M is some finite constant. It is clear that for finite temperatures $\tilde{q}$ has to go to zero as $\Lambda \to 0$.

Thus we have shown that no chiral order exists at finite temperatures in this system. It is easy to extend the proof to the case in which the y or z-component of $Q_{i,j,k}$ is an order parameter. The present proof is also valid even if the Hamiltonian has anisotropy in the y-direction.

Appendix A

Fermionic Representation of the Scalar Chiral Order

The expectation value of the scalar chiral order parameter is given by

$$E_{123} \equiv \langle \sigma_1 \cdot (\sigma_2 \times \sigma_3) \rangle. \tag{A.1}$$

We rewrite the scalar chiral order using the fermion operators c and $c^\dagger$.

$$\begin{aligned} \sigma_1 \cdot (\sigma_2 \times \sigma_3) &= \sigma_1^x(\sigma_2^y\sigma_3^z - \sigma_2^z\sigma_3^y) \\ &\quad +\sigma_1^y(\sigma_2^z\sigma_3^x - \sigma_2^x\sigma_3^z) \\ &\quad +\sigma_1^z(\sigma_2^x\sigma_3^y - \sigma_2^y\sigma_3^x) \qquad \text{(A.2)} \\ &= (\sigma_1^x\sigma_2^y - \sigma_1^y\sigma_2^x)\sigma_3^z \\ &\quad +(\sigma_3^x\sigma_1^y - \sigma_3^y\sigma_1^x)\sigma_2^z \\ &\quad +(\sigma_2^x\sigma_3^y - \sigma_2^y\sigma_3^x)\sigma_1^z \qquad \text{(A.3)} \end{aligned}$$

Using the expression (A.3) and the following relations(A.4),

$$\begin{cases} \sigma_i^x &= \frac{1}{2}(\sigma_i^+ + \sigma_i^-) \\ \sigma_i^y &= \frac{1}{2i}(\sigma_i^+ - \sigma_i^-) \end{cases} \tag{A.4}$$

we obtain

$$\begin{aligned} \frac{i}{2}E_{123} &= \langle \frac{1}{4}(\sigma_1^-\sigma_2^+\sigma_3^z + \sigma_1^+\sigma_3^-\sigma_2^z + \sigma_2^-\sigma_3^+\sigma_1^z - (2 \leftrightarrow 3)) \rangle \\ &= \langle (c_{1\downarrow}^\dagger c_{2\downarrow} c_{2\uparrow}^\dagger c_{3\uparrow} c_{3\uparrow}^\dagger c_{1\uparrow} - c_{1\downarrow}^\dagger c_{3\downarrow} c_{3\downarrow}^\dagger c_{2\downarrow} c_{2\uparrow}^\dagger c_{1\uparrow} \\ &\quad +c_{1\uparrow}^\dagger c_{2\uparrow} c_{2\uparrow}^\dagger c_{3\uparrow} c_{3\downarrow}^\dagger c_{1\downarrow} - c_{1\uparrow}^\dagger c_{3\uparrow} c_{3\downarrow}^\dagger c_{2\downarrow} c_{2\downarrow}^\dagger c_{1\downarrow} \\ &\quad +c_{1\uparrow}^\dagger c_{2\uparrow} c_{2\downarrow}^\dagger c_{3\downarrow} c_{3\uparrow}^\dagger c_{1\uparrow} - c_{1\downarrow}^\dagger c_{3\downarrow} c_{3\uparrow}^\dagger c_{2\uparrow} c_{2\downarrow}^\dagger c_{1\downarrow} \\ &\quad -(2 \leftrightarrow 3)) \rangle \qquad \text{(A.5)} \\ &= (\langle \chi_{12}\chi_{23}\chi_{31} \rangle - \langle \chi_{13}\chi_{32}\chi_{21} \rangle) \qquad \text{(A.6)} \\ &= Pl_{123} - Pl_{132}. \qquad \text{(A.7)} \end{aligned}$$

In the case of the square plaquette(1234) shown in the Fig.A.1, we transform the left hand side of eq.(2.3) in chapter I as follows.

$$\begin{aligned} \chi_{12}\chi_{23}\chi_{34}\chi_{41} - \chi_{14}\chi_{43}\chi_{32}\chi_{21} &= c_{1\alpha}^\dagger c_{2\alpha} c_{2\beta}^\dagger c_{3\beta} c_{3\gamma}^\dagger c_{4\gamma} c_{4\delta}^\dagger c_{1\delta} \\ &\quad -c_{1\alpha'}^\dagger c_{4\alpha'} c_{4\beta'}^\dagger c_{3\beta'} c_{3\gamma'}^\dagger c_{2\gamma'} c_{2\delta'}^\dagger c_{1\delta'} \\ &= c_{1\alpha}^\dagger c_{4\gamma} c_{4\delta}^\dagger c_{3\beta} c_{3\gamma}^\dagger c_{2\alpha} c_{2\beta}^\dagger c_{1\delta} \\ &\quad -c_{1\alpha'}^\dagger c_{4\alpha'} c_{4\beta'}^\dagger c_{3\beta'} c_{3\gamma'}^\dagger c_{2\gamma'} c_{2\delta'}^\dagger c_{1\delta'} \qquad \text{(A.8)} \end{aligned}$$

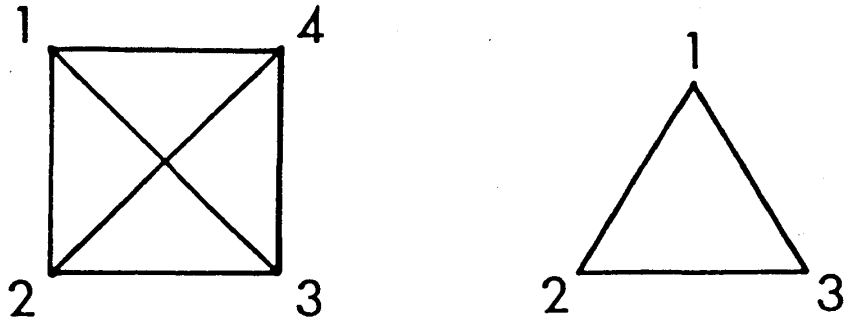

Fig. A.1: Plaquette(123) and Plaquette(1234)

Here Greek indices stand for spin indices and the summations over the same indices are assumed. Among the first terms, the terms arising from the summation with $\alpha = \gamma$ and $\beta = \delta$ are cancelled by the second terms. Thus the terms arising from the summation with $\alpha = -\gamma$ or $\beta = -\delta$ remain non-vanishing and therefore we obtain that

$$\begin{aligned}
\chi_{12}\chi_{23}\chi_{34}\chi_{41} - \chi_{14}\chi_{43}\chi_{32}\chi_{21} &= c^\dagger_{1\alpha}c_{4-\alpha}c^\dagger_{4\beta}c_{3\beta}c^\dagger_{3-\alpha}c_{2\alpha}c^\dagger_{2\beta}c_{1\beta} && \text{(A.9)}\\
&+c^\dagger_{1\alpha}c_{4\alpha}c^\dagger_{4-\beta}c_{3\beta}c^\dagger_{3\alpha}c_{2\alpha}c^\dagger_{2\beta}c_{1-\beta} && \text{(A.10)}\\
&+c^\dagger_{1\alpha}c_{4-\alpha}c^\dagger_{4-\beta}c_{3\beta}c^\dagger_{3-\alpha}c_{2\alpha}c^\dagger_{2\beta}c_{1-\beta} && \text{(A.11)}\\
&-c^\dagger_{1\alpha'}c_{4\alpha'}c^\dagger_{4\beta'}c_{3\beta'}c^\dagger_{3\alpha'}c_{2\alpha'}c^\dagger_{2-\beta'}c_{1-\beta'} && \text{(A.12)}\\
&-c^\dagger_{1\alpha'}c_{4\alpha'}c^\dagger_{4\beta'}c_{3\beta'}c^\dagger_{3-\alpha'}c_{2-\alpha'}c^\dagger_{2\beta'}c_{1\beta'} && \text{(A.13)}\\
&-c^\dagger_{1\alpha'}c_{4\alpha'}c^\dagger_{4\beta'}c_{3\beta'}c^\dagger_{3-\alpha'}c_{2-\alpha'}c^\dagger_{2-\beta'}c_{1-\beta'} && \text{(A.14)}
\end{aligned}$$

Because $\alpha(\alpha')$ is either $\beta(\beta')$ or $-\beta(-\beta')$, the sum of eq.(A.9) and eq.(A.12) can be transformed as follows:

$$\begin{aligned}
\text{Eq.}(A.9) + \text{Eq.}(A.12) &= c_{4-\alpha}c^\dagger_{4-\alpha}c_{3\alpha}c^\dagger_{3-\alpha}(n_{1\alpha}(1-n_{2\alpha}))\\
&+c^\dagger_{1\alpha}c_{1-\alpha}c_{2\alpha}c^\dagger_{2-\alpha}(1-n_{4-\alpha})(1-n_{3-\alpha})\\
&-c_{4\alpha'}c^\dagger_{4-\alpha'}c_{3-\alpha'}c^\dagger_{3\alpha'}(n_{1\alpha'}(1-n_{2\alpha'})\\
&-c^\dagger_{1\alpha'}c_{1-\alpha'}c_{2\alpha'}c^\dagger_{2-\alpha'}(1-n_{4\alpha'})(1-n_{3\alpha'}) && \text{(A.15)}\\
&= c^\dagger_{1\alpha}c_{1-\alpha}c_{2\alpha}c^\dagger_{2-\alpha}\{(1-n_{4-\alpha})(1-n_{3-\alpha})\\
&-(1-n_{4\alpha})(1-n_{3\alpha})\}\\
&+c_{4-\alpha}c^\dagger_{4\alpha}c_{3\alpha}c^\dagger_{3-\alpha}\{n_{1\alpha}(1-n_{2\alpha})\\
&-n_{1-\alpha}(1-n_{2-\alpha})\}. && \text{(A.16)}
\end{aligned}$$

Using the following relations

$$(1-n_{4-\alpha})(1-n_{3-\alpha}) - (1-n_{4\alpha})(1-n_{3\alpha})$$

$$
\begin{aligned}
&= \frac{1}{2}[(1-n_{4-\alpha})(1-n_{3-\alpha})+(1-n_{4\alpha})(1-n_{3-\alpha}) \\
&\quad -(1-n_{4\alpha})(1-n_{3\alpha})-(1-n_{4\alpha})(1-n_{3-\alpha}) \\
&\quad +(1-n_{4-\alpha})(1-n_{3-\alpha})+(1-n_{4-\alpha})(1-n_{3\alpha}) \\
&\quad -(1-n_{4\alpha})(1-n_{3\alpha})-(1-n_{4-\alpha})(1-n_{3\alpha})] \\
&= (1-n_{3-\alpha})-(1-n_{4\alpha})+(1-n_{4-\alpha})-(1-n_{3\alpha}), \qquad \text{(A.17)}
\end{aligned}
$$

we obtain

$$
\begin{aligned}
&\text{Eq.}(A.9)+\text{Eq.}(A.12) \\
&= \frac{1}{2}[c^\dagger_{1\alpha}c_{1-\alpha}c_{2\alpha}c^\dagger_{2-\alpha}\{c_{3-\alpha}c^\dagger_{3-\alpha}-c_{4\alpha}c^\dagger_{4\alpha}+c_{4-\alpha}c^\dagger_{4-\alpha}-c_{3\alpha}c^\dagger_{3\alpha}\}] \\
&\quad +\frac{1}{2}[c_{4-\alpha}c^\dagger_{4\alpha}c_{3\alpha}c^\dagger_{3-\alpha}\{c_{2\alpha}c^\dagger_{2\alpha}-c^\dagger_{1-\alpha}c_{1-\alpha}+c^\dagger_{1\alpha}c_{1\alpha}-c_{2-\alpha}c^\dagger_{2-\alpha}\}] \qquad \text{(A.18)} \\
&= \frac{1}{2}[c^\dagger_{1\alpha}c_{2\alpha}c^\dagger_{2-\alpha}c_{3-\alpha}c^\dagger_{3-\alpha}c_{1-\alpha}\cdots(\text{one of the elements of } Pl_{123}) \\
&\quad -c^\dagger_{1\alpha}c_{4\alpha}c^\dagger_{4\alpha}c_{2\alpha}c^\dagger_{2-\alpha}c_{1-\alpha}\cdots(\text{one of the elements of } Pl_{142}) \\
&\quad +c^\dagger_{1\alpha}c_{2\alpha}c^\dagger_{2-\alpha}c_{4-\alpha}c^\dagger_{4-\alpha}c_{1-\alpha}\cdots(\text{one of the elements of } Pl_{124}) \\
&\quad -c^\dagger_{1\alpha}c_{3\alpha}c^\dagger_{3\alpha}c_{2\alpha}c^\dagger_{2-\alpha}c_{1-\alpha}\cdots(\text{one of the elements of } Pl_{132}) \\
&\quad -c^\dagger_{4\alpha}c_{2\alpha}c^\dagger_{2\alpha}c_{3\alpha}c^\dagger_{3-\alpha}c_{4-\alpha}\cdots(\text{one of the elements of } Pl_{423}) \\
&\quad -c^\dagger_{1-\alpha}c_{4-\alpha}c^\dagger_{4\alpha}c_{3\alpha}c^\dagger_{3-\alpha}c_{1-\alpha}\cdots(\text{one of the elements of } Pl_{143}) \\
&\quad +c^\dagger_{1\alpha}c_{3\alpha}c^\dagger_{3-\alpha}c_{4-\alpha}c^\dagger_{4\alpha}c_{1\alpha}\cdots(\text{one of the elements of } Pl_{134}) \\
&\quad +c^\dagger_{4\alpha}c_{3\alpha}c^\dagger_{3-\alpha}c_{2-\alpha}c^\dagger_{2-\alpha}c_{4-\alpha} \\
&\qquad \cdots(\text{one of the elements of } Pl_{432})]. \qquad \text{(A.19)}
\end{aligned}
$$

Where $n_{i\sigma} \equiv c^\dagger_{i\sigma}c_{i\sigma}$ and we have used the constraint $\sum_\sigma n_{i\sigma}=1$. In the same way we obtain the following relations:

$$
\begin{aligned}
&\text{Eq.}(A.10)+\text{Eq.}(A.13) \\
&\quad = \frac{1}{2}[c^\dagger_{1\alpha}c_{2\alpha}c^\dagger_{2-\alpha}c_{3-\alpha}c^\dagger_{3\alpha}c_{1\alpha}-c^\dagger_{1\alpha}c_{4\alpha}c^\dagger_{4-\alpha}c_{2-\alpha}c^\dagger_{2-\alpha}c_{1-\alpha} \\
&\quad +c^\dagger_{1\alpha}c_{2\alpha}c^\dagger_{2\alpha}c_{4\alpha}c^\dagger_{4-\alpha}c_{1-\alpha}-c^\dagger_{1-\alpha}c_{3-\alpha}c^\dagger_{3\alpha}c_{2\alpha}c^\dagger_{2-\alpha}c_{1-\alpha} \\
&\quad -c^\dagger_{4\alpha}c_{2\alpha}c^\dagger_{2-\alpha}c_{3-\alpha}c^\dagger_{3\alpha}c_{4\alpha}-c^\dagger_{1\alpha}c_{4\alpha}c^\dagger_{4-\alpha}c_{3-\alpha}c^\dagger_{3-\alpha}c_{1-\alpha} \\
&\quad +c^\dagger_{1\alpha}c_{3\alpha}c^\dagger_{3\alpha}c_{4\alpha}c^\dagger_{4-\alpha}c_{1-\alpha}+c^\dagger_{4-\alpha}c_{3-\alpha}c^\dagger_{3\alpha}c_{2\alpha}c^\dagger_{2-\alpha}c_{1-\alpha}] \qquad \text{(A.20)}
\end{aligned}
$$

and

$$
\begin{aligned}
&\text{Eq.}(A.11)+\text{Eq.}(A.14) \\
&\quad = \frac{1}{2}[c^\dagger_{1\alpha}c_{2\alpha}c^\dagger_{2\alpha}c_{3\alpha}c^\dagger_{3-\alpha}c_{1-\alpha}-c^\dagger_{1-\alpha}c_{4-\alpha}c^\dagger_{4\alpha}c_{2\alpha}c^\dagger_{2-\alpha}c_{1-\alpha}
\end{aligned}
$$

$$
\begin{aligned}
&+c^\dagger_{1\alpha}c_{2\alpha}c^\dagger_{2-\alpha}c_{4-\alpha}c^\dagger_{4\alpha}c_{1\alpha} - c^\dagger_{1\alpha}c_{3\alpha}c^\dagger_{3-\alpha}c_{2-\alpha}c^\dagger_{2-\alpha}c_{1-\alpha} \\
&-c^\dagger_{4\alpha}c_{2\alpha}c^\dagger_{2-\alpha}c_{3-\alpha}c^\dagger_{3-\alpha}c_{4-\alpha} - c^\dagger_{1\alpha}c_{4\alpha}c^\dagger_{4\alpha}c_{3\alpha}c^\dagger_{3-\alpha}c_{1-\alpha} \\
&+c^\dagger_{1\alpha}c_{3\alpha}c^\dagger_{3-\alpha}c_{4-\alpha}c^\dagger_{4-\alpha}c_{1-\alpha} + c^\dagger_{4\alpha}c_{3\alpha}c^\dagger_{3\alpha}c_{2\alpha}c^\dagger_{2-\alpha}c_{4-\alpha}]. \qquad \text{(A.21)}
\end{aligned}
$$

From eq.(A.19), eq.(A.20) and eq.(A.21), we arrive finally at the relation

$$
\begin{aligned}
\langle\chi_{12}\chi_{23}\chi_{34}\chi_{41}\rangle - \langle\chi_{14}\chi_{43}\chi_{32}\chi_{21}\rangle &= \frac{1}{2}[Pl_{123} - Pl_{132} + Pl_{124} - Pl_{142} \\
&\quad +Pl_{134} - Pl_{143} + Pl_{432} - Pl_{423}] \qquad \text{(A.22)} \\
&= \frac{i}{4}[E_{123} + E_{124} + E_{134} - E_{234}]. \qquad \text{(A.23)}
\end{aligned}
$$

Appendix B

Properties of the Scalar Chiral Order X_{ijk}

The scalar chiral operator X_{123} is expressed by

$$
X_{123} = \frac{1}{8}\sigma_1 \cdot (\sigma_2 \times \sigma_3). \qquad \text{(B.1)}
$$

Then the square of X is

$$
\begin{aligned}
X^2_{123} &= \frac{1}{64}(\sigma_1 \cdot (\sigma_2 \times \sigma_3))^2 \\
&= \frac{1}{64}\{\sigma^x_1(\sigma^y_2\sigma^z_3 - \sigma^z_2\sigma^y_3) + \sigma^y_1(\sigma^z_2\sigma^x_3 - \sigma^x_2\sigma^z_3) + \sigma^z_1(\sigma^x_2\sigma^y_3 - \sigma^y_2\sigma^x_3)\}^2 \qquad \text{(B.2)}
\end{aligned}
$$

Using the following algebra of the Pauli matrices

$$
(\sigma^k)^2 = 1 \quad k = x, y, z, \qquad \text{(B.3)}
$$

$$
\sigma^i\sigma^j = i\epsilon_{ijk}\sigma^k \quad , \quad \epsilon_{123} = 1 \qquad \text{(B.4)}
$$

we obtain

$$
\begin{aligned}
(\sigma^x_1(\sigma^y_2\sigma^z_3 - \sigma^z_2\sigma^y_3))^2 &= (\sigma^y_2\sigma^z_3 - \sigma^z_2\sigma^y_3)^2 \\
&= 2 - \sigma^y_2\sigma^z_2\sigma^z_3\sigma^y_3 - \sigma^z_2\sigma^y_2\sigma^y_3\sigma^z_3 \\
&= 2 - 2\sigma^x_2\sigma^x_3 \qquad \text{(B.5)}
\end{aligned}
$$

and

$$
\begin{aligned}
&\sigma^x_1\sigma^y_2(\sigma^y_2\sigma^z_3 - \sigma^z_2\sigma^y_3)(\sigma^z_2\sigma^x_3 - \sigma^x_2\sigma^z_3) \\
&= i\sigma^z_1\{(i\sigma^x_2)(i\sigma^y_3) - (-i\sigma^z_2) - (-i\sigma^z_3) + (i\sigma^y_2)(i\sigma^x_3)\} \\
&= -\sigma^z_1\sigma^z_2 - \sigma^z_1\sigma^z_3 - i\sigma^z_1(\sigma^x_2\sigma^y_3 + \sigma^y_2\sigma^z_3). \qquad \text{(B.6)}
\end{aligned}
$$

Substituting eq.(B.5) and eq.(B.6) into eq.(B.2), we finally obtain

$$\begin{aligned} X_{123}^2 &= \frac{1}{64}\{6-2(\sigma_1\cdot\sigma_2+\sigma_2\cdot\sigma_3+\sigma_3\cdot\sigma_1)\} \\ &= \frac{1}{64}\{15-(\sigma_1+\sigma_2+\sigma_3)^2\} \\ &= \frac{15}{64}-\frac{1}{16}(\boldsymbol{S}_1+\boldsymbol{S}_2+\boldsymbol{S}_3)^2 \end{aligned} \tag{B.7}$$

Next we consider the commutation relation between the chiral order X and the total spin $\boldsymbol{S}$. As $\{X_{123}\}$ have the following symmetry property :

$$X_{123}=X_{231}=X_{312}, \tag{B.8}$$

we can write $[S_j^z, X_{123}]$ for j=1,2,3 as follows:

$$\begin{aligned} [S_1^z, X_{123}] &= [S_1^z, S_1^x(\boldsymbol{S}_2\times\boldsymbol{S}_3)^x+S_1^y(\boldsymbol{S}_2\times\boldsymbol{S}_3)^y] \\ &= iS_1^y(\boldsymbol{S}_2\times\boldsymbol{S}_3)^x+(-i)S_1^x(\boldsymbol{S}_2\times\boldsymbol{S}_3)^y \end{aligned} \tag{B.9}$$

$$[S_2^z, X_{123}] = [S_2^z, X_{231}] = iS_2^y(\boldsymbol{S}_3\times\boldsymbol{S}_1)^x+(-i)S_2^x(\boldsymbol{S}_3\times\boldsymbol{S}_1)^y \tag{B.10}$$

$$[S_3^z, X_{123}] = [S_3^z, X_{312}] = iS_3^y(\boldsymbol{S}_1\times\boldsymbol{S}_2)^x+(-i)S_3^x(\boldsymbol{S}_1\times\boldsymbol{S}_2)^y. \tag{B.11}$$

Thus some easy calculations show that

$$[S_1^z+S_2^z+S_3^z, X_{123}]=0. \tag{B.12}$$

From the symmetry of X, we obtain

$$[\boldsymbol{S}, X_{123}]=0 \tag{B.13}$$

where $\boldsymbol{S}=\boldsymbol{S}_1+\boldsymbol{S}_2+\boldsymbol{S}_3$ is the total spin.

Appendix C

Analytic Results in a System of Four Spins

In the systems of four spins, we can easily diagonalize the Hamiltonian(4.2) (see the Table I.1). Thus we get the following results.

From the Table I.1, the partition function Z of the relevant Hamiltonian is given by

$$\begin{aligned} Z &= 6\exp(-\beta(-\frac{t}{2}))+5\exp(-\beta(\frac{t}{2}+1))+3\exp(-\beta(\frac{t}{2}-1)) \\ &\quad +\exp(-\beta(\frac{t}{2}-2))+\exp(-\beta(-\frac{3}{2}t)), \end{aligned} \tag{C.1}$$

#	$\langle X_{123}X_{234}\rangle$	$\langle X_{123}X_{341}\rangle$	$\langle X_{123}^2\rangle$	Eigenvalues
1	0	0	0	$t/2+1$
2	0	0	0	$t/2+1$
3	$(1/16)(1-i)$	0	1/8	$-t/2$
4	0	-1/8	1/8	$t/2-1$
5	$(1/16)(1+i)$	0	1/8	$-t/2$
6	$(-3/16)$	3/16	3/16	$t/2-2$
7	0	0	0	$t/2+1$
8	$(1/16)(1-i)$	0	1/8	$-t/2$
9	$-(3/16)$	3/16	3/16	$-3t/2$
10	$(1/16)(1+i)$	0	1/8	$-t/2$
11	0	-1/8	1/8	$t/2-1$
12	0	0	0	$t/2+1$
13	$(1/16)(1-i)$	0	1/8	$-t/2$
14	0	-1/8	1/8	$t/2-1$
15	$(1/16)(1+i)$	0	1/8	$-t/2$
16	0	0	0	$t/2+1$

Table C.1: The expectation values of $X_{123}X_{234}$, $X_{123}X_{341}$ and X_{123}^2 for each eigenstate of $\mathcal{H}$.

where $\beta = (k_BT)^{-1}$. From the Table C.1, the expectation values of $X_{123}X_{234}$, $X_{123}X_{341}$ and X_{123}^2 are given as follows:

$$\langle X_{123}X_{234}\rangle Z = \frac{3}{8}\exp(-\beta(-\frac{t}{2})) - \frac{3}{16}(\exp(-\beta(\frac{t}{2}-2)) + \exp(\beta\frac{3t}{2})) \quad \text{(C.2)}$$

$$\langle X_{123}X_{341}\rangle Z = -\frac{3}{8}\exp(-\beta(\frac{t}{2}-1)) + \frac{3}{16}(\exp(-\beta(\frac{t}{2}-2)) + \exp(\beta\frac{3t}{2})) \quad \text{(C.3)}$$

$$\langle X_{123}^2\rangle Z = \frac{3}{4}\exp(-\beta(-\frac{t}{2})) + \frac{3}{8}\exp(-\beta(\frac{t}{2}-1)) + \frac{3}{16}(\exp(-\beta(\frac{t}{2}-2)) + \exp(-\beta(-\frac{3t}{2}))). \quad \text{(C.4)}$$

It follows from eqs.(C.2), (C.3) and (C.4) that

$$\langle X_{123}X_{234}\rangle \to 0 \quad \text{as} \quad T \to \infty$$

$$\langle X_{123}X_{234}\rangle \to -\frac{3}{16} \quad \text{as} \quad T \to 0$$

$$\langle X_{123}X_{341}\rangle \to 0 \quad \text{as} \quad T \to \infty$$

$$\langle X_{123}X_{341}\rangle \to \frac{3}{16} \quad \text{as} \quad T \to 0$$

$$\langle X_{123}^2 \rangle \to \frac{3}{32} \quad \text{as} \quad T \to \infty$$
$$\langle X_{123}^2 \rangle \to \frac{3}{16} \quad \text{as} \quad T \to 0$$

and

$$\langle X_{123} X_{234} \rangle < 0$$
$$\langle X_{123} X_{341} \rangle > 0$$

for any T and t.

References

[1] J. A. Bednorz and K. A. Muller, Z. Phys. B64 (1986) 189.

[2] W. G. Wen, F. Wilczek and A. Zee, Phys. Rev. B39 (1989) 11413.

[3] Y. H. Chen, F. Wilczek, E. Witten and B. I. Halperin, Int. J. Modern Phys. B3 (1989) 1001.

[4] M. Suzuki, J. Phys. Soc. Jpn. 57 (1988) 2310.

[5] N. Kawashima and M. Suzuki, J. Phys. Soc. Jpn. 58 (1989) 3123.

[6] M. Suzuki, J. de Phys. (Paris) Colloque C8 (1988) 1519

[7] M. Suzuki, J. Phys. Soc. Jpn. 55 (1986) 4205.

[8] M. Suzuki, M. Katori and X. Hu, J. Phys. Soc. Jpn. 56 (1987) 3092.

[9] G. Baskaran, Phys. Rev. Lett. 63 (1989) 2524.

[10] M. Imada, J. Phys. Soc. Jpn. 58 (1989) 2650.

[11] E. Dagotto and A. Moreo, Phys. Rev. Lett. 63 (1989) 2148.

[12] J. Villain, J. Phys. C10 (1977) 1717 and 4793;
G. Forgacs, Phys. Rev. B22 (1980) 4473;
D. H. Lee, R. G. Caflish, J. D. Joannopoulos and F. Y. Wu, Phys. Rev. B29 (1984) 2680.

[13] S. Teitel and C. Jayaprakash, Phys. Rev. B27 (1983) 598.

[14] S. Miyashita and H. Shiba, J. Phys. Soc. Jpn. 53 (1984) 1145.

[15] D. H. Lee, J. D. Joannopoulos, J. W. Negele and D. P. Landau, Phys. Rev. Lett. 52 (1984) 433; Phys. Rev. B33 (1986) 450.

[16] B. Berge, H. T. Diep, A. Ghazali and P. Lallemand, Phys. Rev. B34 (1986) 3177.

[17] S. Fujiki and D. D. Betts, Can. J. Phys. 64 (1986) 876; *ibid.* 65 (1987) 76; S. Fujiki, Can. J. Phys. 65 (1987) 489.

[18] S. Fujiki and D. D. Betts, Prog. Theor. Phys. Suppl. No. 87 (1986) 268.

[19] H. Nishimori and H. Nakanishi, J. Phys. Soc. Jpn. 57 (1988) 626; S. Miyashita, J. Phys. Soc. Jpn. 57 (1988) 1934.

[20] F. Matsubara and S. Inawashiro, Solid State Commun. 67 (1988) 229.

[21] N. D. Mermin and H. Wagner, Phys. Rev. Lett. 17 (1966) 1133; P. C. Hohenberg, Phys. Rev. 158 (1967) 383.